9th ANKARA INTERNATIONAL AEROSPACE CONFERENCE AIAC-2017-179
20-22 September 2017 - METU, Ankara TURKEY

ICING ON WIND TURBINE BLADE UNDER VARIOUS ATMOSPHERIC CONDITIONS

Özcan Yırtıcı*, İsmail H. Tuncer† and Serkan Özgen‡
METU
Ankara, Turkey

ABSTRACT

It is important to predict the ice shape with amount of accreted mass on the surface of turbine blade in order to design and develop de/anti-icing systems for wind turbines located in cold climate regions. Ice accretion on the blades change the initial shape and this cause alteration in the aerodynamic characteristic of the blades. To this end, icing module combined with the BEM method to predict the shape of the iced blade sections of the turbine blade under atmospheric icing conditions. The obtained results are verified with experimental and numerical ice shapes reported in the literature. In all the cases studied, the current numerical tool yields results that are in fair agreement with the compared results and can be used to predict ice accretion on wind turbine's blades under atmospheric icing conditions.

INTRODUCTION

The renewable energy has been significant since the global warming has caused climate changes in recent years. Therefore utilizing of wind energy has gained importance and installation of wind turbines in the world has been increasing in a steady manner. About three percent of the world's electricity is delivered by wind power. This share is expected to grow to 7.3 percent by 2018 according to Navigant Research [Navigant, 2015]. Wind resources in cold climate regions and mountainous areas are typically good and making them attractive for wind energy. However especially in winter, the wind turbines are exposed to heavy atmospheric icing conditions. In the horizontal axis wind turbines, aerodynamic performance losses are similar to that observed by wings and helicopter rotors under icing conditions [Jasinski, 1998]. Atmospheric icing causes power losses since ice accretion on blades changes the clean blade aerodynamic characteristics and creates instrument or controller errors on wind turbines. The amount of wind power losses depend on the amount of ice accumulation on the blades, blade design and turbine control. Therefore, evaluating the impact of ice accretion on wind turbine performance losses is important since the poor turbine selection results in a financially sub-optimal investment.

Numerical modeling of ice accretion and its effects on wind turbine performance has been studied by many researchers in recent years. Aerodynamic performance degradation can reduce the power

*GRA. in a Aerospace Engineering Department, Email: oyirtici@ae.metu.edu.tr
†Prof in a Aerospace Engineering Department, Email: ismail.h.tuncer@ae.metu.edu.tr
‡Prof in a Aerospace Engineering Department, Email: serkan.ozgen@ae.metu.edu.tr

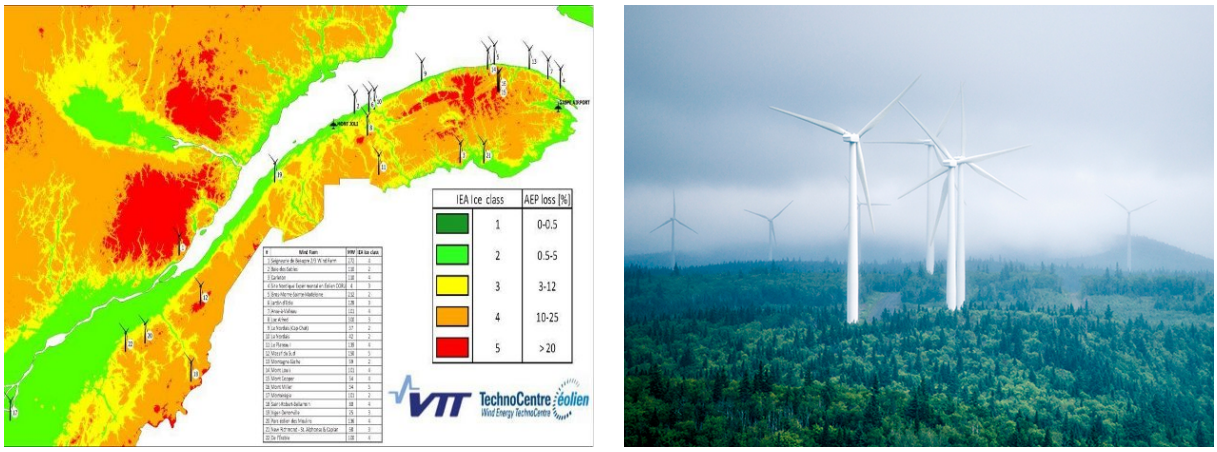

(a) Icing map of Quebec [VTT, 2017]

(b) Wind farm, Quebec (Photo: iStockphoto)

Figure 1: Wind farms located in cold climate region

coefficient in the range of $20 - 50\%$ [Talhaug, 2007] and the annual energy production (AEP) by up to 17% [Barber, 2011]. For this reason, the international energy agency (IEA) announced Annex XIX: "Wind Energy in Cold Climates" to predict better the effect of ice accretion on energy production [IEAWind, 2015]. In Figure 1, one of the view of a wind farm located in cold climate region with frequency of icing event are given for Quebec, Canada. In order to prevent or mitigate icing effects on wind turbine active or passive anti-icing and de-icing systems (ADIS) can be used, but few are available on the market. ADIS are generally based on heating, therefore wind turbines need more power to operate. Although early power consumptions of ADIS electrical heating were $\approx$ 25 % of the nominal power output of the given turbine, with the advances in technology this consumption is reduced to $\approx$ 2 % of nominal power output. Nowadays ADIS use up 4 % of the annual energy production depending on icing severity [Parent, 2011]. Icing modeling can aid in the positioning of ADIS to reduce energy consumption needed to operate these devices.

In order to maximize energy production from the turbine which is operating under icing conditions performance losses needed to be predicted. Fluid flow simulation that predicts ice formation on turbine blades can help maintain safety, reduce performance losses and decrease weight.

METHODOLOGY

Icing modeling makes it possible to obtain data for generating ice shapes for geometries like aircraft, transmission line wires, etc. under a wide range of simulation conditions. Icing module is used to predict icing shape geometry at given blade sections on the wind turbine blade. The main inputs to this module are blade section geometry, flow conditions (free stream velocity, angle of attack, etc.) and weather conditions (temperature, MVD, LWC, exposure time, etc.). The main outputs are sectional ice shape geometry and corresponding aerodynamic coefficients.

Ice accretion prediction involves complex physics comprising aerodynamics, heat transfer and multiphase flow, which are all time dependent and involve geometric deformation. The numerical method employed in this study predicts the ice accretion on aerodynamic surfaces as a result of water droplets hitting on the surface iteratively. It employs the general methodology for the simulation of ice accretion on airfoils, which is based on the successive calculation of air flow, water droplet trajectories, collection efficiency, heat transfer balance and accreted ice. Four main modules used in this study are briefly explained.

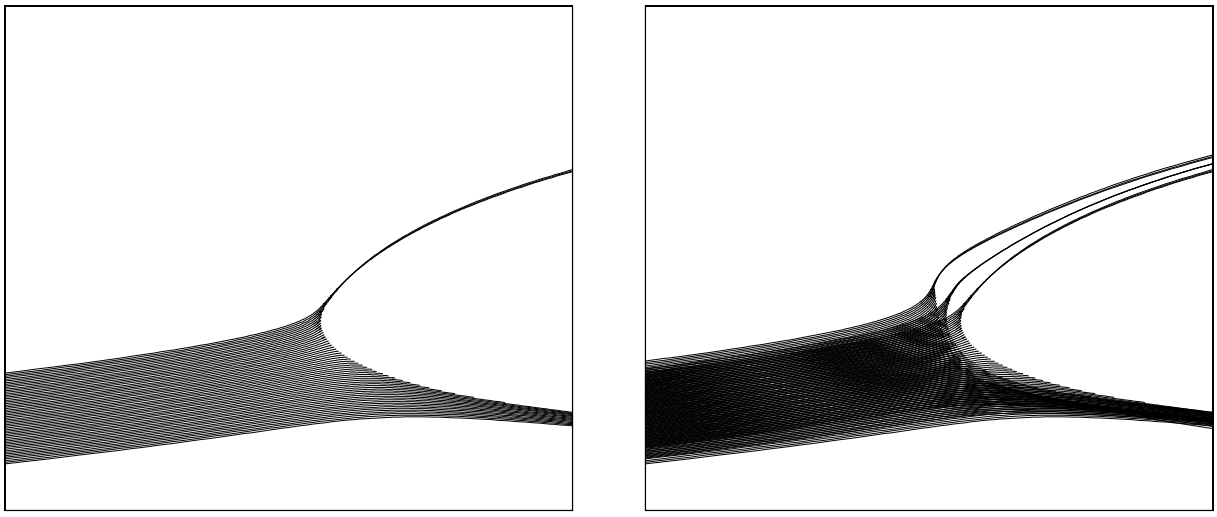

(a) 1 layer (b) 3 layers

Figure 2: Particle trajectories for a NACA 0012 airfoil for 7 mins icing time

Flow Field Solution

In order to obtain the flow field velocity components required for droplet trajectory calculations, a panel code coupled with a turbulent boundary Layer module is used. This potential flow solver provides the external velocity distribution to determine the convective heat transfer coefficients in thermodynamic analysis in icing computations. In order to obtain more accurate sectional aerodynamic loads in the BEM formulation (especially the drag coefficient), flow over clean and iced blade profiles are solved by XFOIL [XFOIL, 2017]. It is an open source software used for the design and analysis of subsonic airfoils. XFOIL implements a linear-vorticity second order accurate panel method, and is coupled with an integral boundary-layer method and an $e^n - type$ transition prediction formulation.

Calculation of Droplet Trajectories and Collection Efficiency

Droplet trajectories are computed by using a Langrangian approach to obtain the collection efficiency distribution around the blade sections. Typical droplet trajectories are illustrated in Figure 2. The droplet impact distribution on the airfoil determines the impingement limits and the distribution of water mass on the airfoil. For droplet trajectories, the following assumptions are employed :

- Droplets are assumed to be spherical.
- The flow field is not affected by the presence of the droplets.
- Gravity and aerodynamic drag are the only forces acting on the droplets.

Droplet trajectories are computed with the following equations :

$$m\ddot{x_p} = -Dcos\gamma$$

$$m\ddot{y_p} = -Dsin\gamma + mg$$

with :

$$\gamma = tan^{-1}\frac{\dot{y_p} - V_y}{\dot{x_p} - V_x}$$

$$D = \frac{1}{2}\rho V_{rel}^2 C_D A_P$$

$$V_{rel} = \sqrt{(\dot{x_p} - V_x)^2 + (\dot{y_p} - V_y)^2}$$

In the above equations, V_x and V_y are the flow velocity components at the droplet location, while $\dot{x_p}$, $\dot{y_p}$, $\ddot{x_p}$ and $\ddot{y_p}$ are the components of the droplet velocity and acceleration. Atmospheric density is denoted by ρ, while droplet cross-sectional area and drag coefficient are represented by A_p and C_D respectively. Droplet drag coefficients are computed using an empirical drag law based on the droplet Reynolds number [Ozgen, 2009]. The droplet trajectories are obtained with the integration of the first two equations over time until the impact of the droplets to the geometry occurs. The local collection efficiency (β) is defined as the ratio of the area of impingement to the area through which water passes at some distance upstream of the section.

Extended Messinger Method

To determine the thickness of ice, convective heat transfer coefficients are determined by using the two-dimensional Integral Boundary Layer equation and the thermodynamic balance is achieved with the Extended Messinger model. Extended Messinger Model is governed by four equations; energy equations in ice and water layers, a mass balance and a phase change or Stefan condition at the ice/water interface [Myers, 2001].

$$\frac{\partial T}{\partial t} = \frac{k_i}{\rho_i C p_i}\frac{\partial^2 T}{\partial y^2} \tag{1}$$

$$\frac{\partial \theta}{\partial t} = \frac{k_w}{\rho_w C p_w}\frac{\partial^2 \theta}{\partial y^2} \tag{2}$$

$$\rho_i \frac{\partial B}{\partial t} + \rho_w \frac{\partial h}{\partial t} = \rho_a \beta V_\infty \tag{3}$$

$$\rho_i L_F \frac{\partial B}{\partial t} = k_i \frac{\partial T}{\partial y} - k_w \frac{\partial \theta}{\partial y} \tag{4}$$

where θ and T are the temperatures, k_i and k_w are thermal conductives, Cp_i and Cp_w are the specific heats and h and B are the thickness of water and ice layers, respectively. In equation 3, $\rho_a \beta V_\infty$ is impinging water mass flow rates for a panel, respectively. Meanwhile, ρ_i and L_F refer the density of ice and the latent heat of solidification of water. In order to determine the ice and water thicknesses together with the temperature distribution at each layer, boundary and initial conditions must be specified. These are based on the following assumptions [Myers, 2001]:

- Ice is in perfect contact with the airfoil surface, which is taken to be equal to the air temperature, T_a:

$$T(0,t) = T_s \tag{5}$$

- The temperature is continuous at the ice/water boundary and is equal to the freezing temperature:

$$T(B,t) = \theta(B,t) = T_f \tag{6}$$

- At the air/water (glaze ice) or air/ice (rime ice) interface, heat flux is determined by convection (Q_c), radiation (Q_r), latent heat release (Q_l), cooling by incoming droplets (Q_d), heat brought in by runback water (Q_{in}), evaporation (Q_e) or sublimation (Q_s), aerodynamic heating(Q_a) and kinetic energy of incoming droplets (Q_k):

$$For\ glaze\ ice: \quad -k_w \frac{\partial \theta}{\partial y} = (Q_c + Q_e + Q_d + Q_r) - (Q_a + Q_k + Q_{in}) \ \ at\ y = B + h \tag{7}$$

$$For\ rime\ ice: \quad -k_i \frac{\partial T}{\partial y} = (Q_c + Q_s + Q_d + Q_r) - (Q_a + Q_k + Q_{in} + Q_l) \ \ at\ y = B \tag{8}$$

- Airfoil surface is initially clean:

$$B = h = 0, \quad t = 0 \tag{9}$$

These equations are written for each panel and ice is assumed to grow perpendicularly to a panel.

BEM Methodology

The BEM methodology is used widely in wind turbine design and performance analysis due to its accuracy and ease of implementation. Blade is divided into the finite elements along the span and 2D solutions in each section is used to reconstruct the 3D flow field and the loading on the blade. BEM module provide the value of sectional velecities and angles of attack to predict ice shape for each blade element.

RESULTS AND DISCUSSION

Validation Case: Ice Accretion Prediction over NACA 0012 Wing Profile

The present method developed is first validated against the numerical study over NACA 0012 airfoil performed by Makkonen et al.[Makkonen, 2001]. The geometric and flow conditions in the reference study are presented in Table 1.

Table 1: Geometric characteristics and flow conditions used in the calculations

Variables	Value
Ambient temperature, T_a	-27.8, -19.8, -16.7 -13.9, -6.7, -3.9, -2.9 °C
Freestream velocity, V_∞	58.1, 102.8 m/s
Airfoil chord , c	0.53 m
Liquid water content, ρ_a	0.55, 1.3 g/m^3
Droplet diameter, d_p	20 μ m
Exposure time, t_{exp}	7, 8 mins
Ambient pressure, p_∞	95610 Pa
Angle of attack, α	3.5, 4.0°
Humidity	100 %

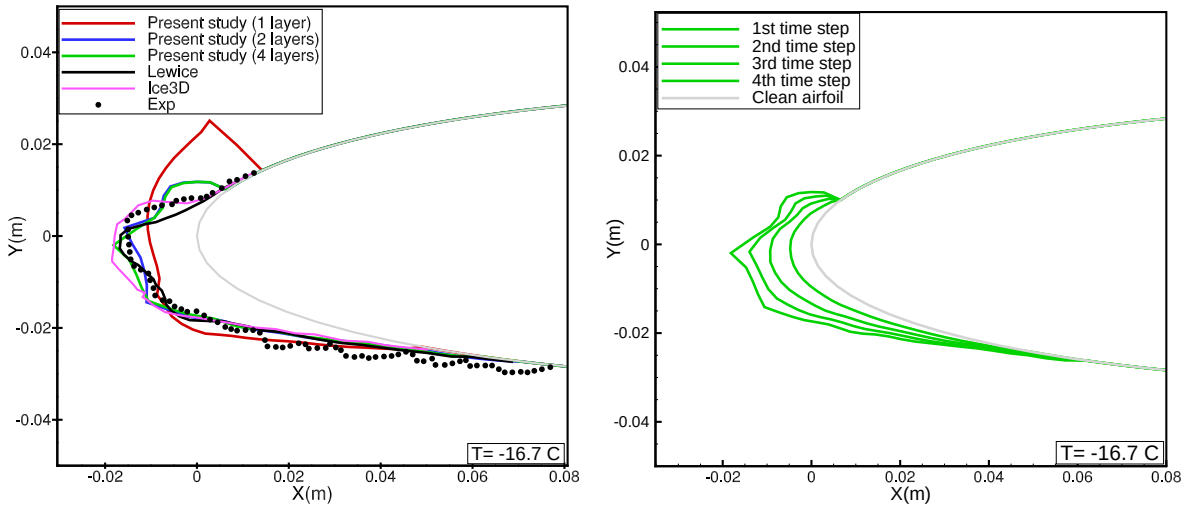

Figure 3: Predicted ice shapes for NACA 0012 airfoil for conditions in Table 1 (V_∞= 102 m/s, α= 3.5°, ρ_a=0.55 g/m^3 and t_{exp}=7 mins)

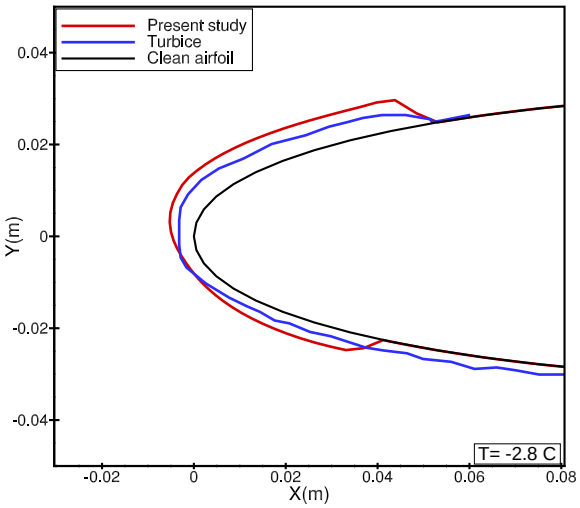

(a) Glaze ice

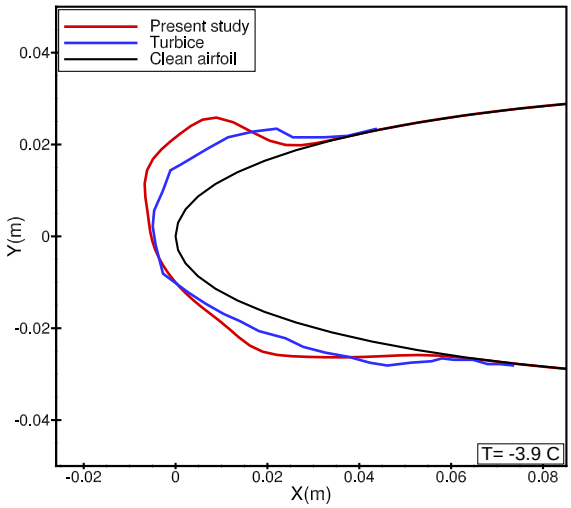

(b) Glaze ice

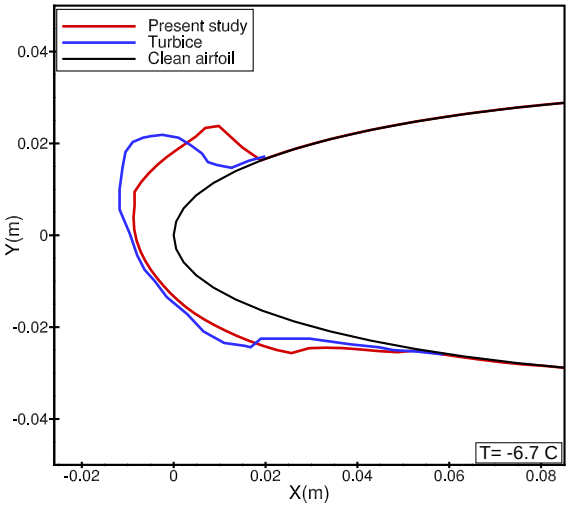

(c) Glaze ice

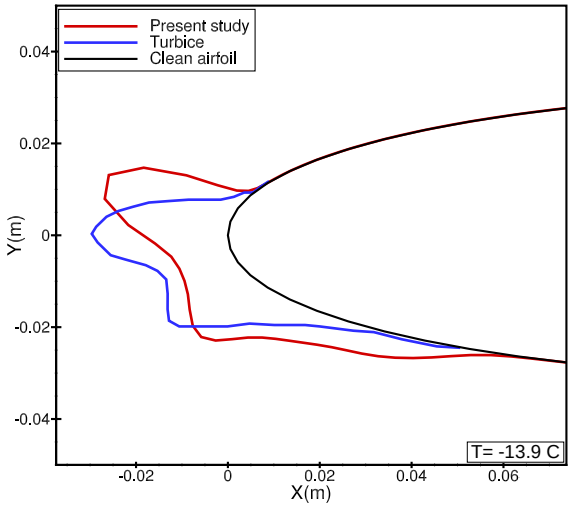

(d) Rime ice

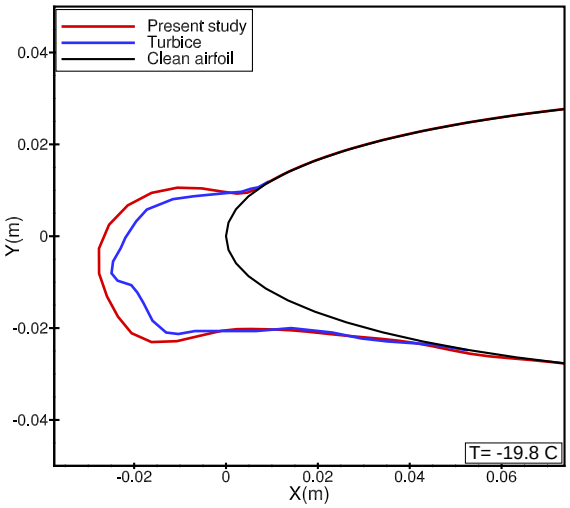

(e) Rime ice

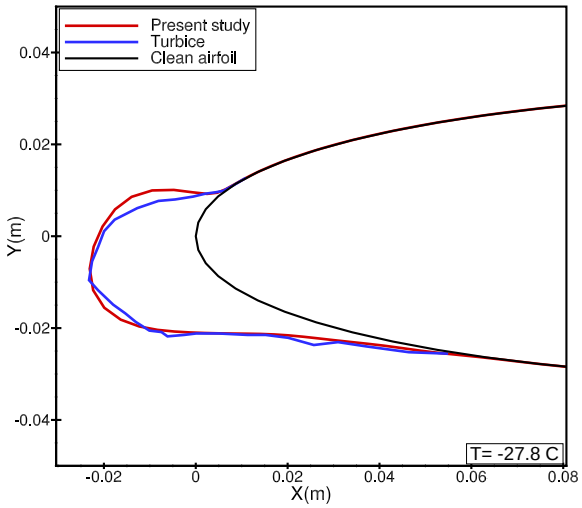

(f) Rime ice

Figure 4: Predicted ice shapes for NACA 0012 a profile for conditions in Table 1 (V_∞= 58.1 m/s, α= 4.0°, ρ_a=1.3 g/m^3 and t_{exp}=8 mins)

In Figure 4, obtained ice shapes are compared with those predicted numerically by Turbice respectively. It is observed that all the predictions agree fairly well. Present solver predicts bigger ice shape than Turbice in glaze ice conditions. In rime ice conditions, except the shape of horn obtained for -13.9 °C rime ice shapes agree rather well. Atmospheric pressure, runback water, humidty, break up, splash effects are the information which are missing may cause this discrepancy.

Effect of Temperature and Droplet Size on Ice Shape

In this case, ice accretion prediction code was used to predict 2D ice profile shapes on the blade at 16 different span-wise locations for the Aeolos-H 30kW wind turbine under different atmospheric icing conditions to investigate the effects of temperature and droplet size on ice accretion. The obtained 2D iced profiles are extrapolated to to generate 3D iced turbine blade. The geometric and flow conditions in the reference study are presented in Table 2.

Table 2: Parameters used to define icing profiles

Airfoils	DU93-W-210
Rotational speed	120 rpm
Rated speed	11 m/s
Root chord	0.703 m
Tip chord	0.02 m
Turbine diameter ,R	12 m
Twist	17.45 degrees (max.)
Mode of control	variable speed/yawing
Liquid water content, ρ_a	0.05 g/m^3
Droplet diameter, d_p	27, 35 μ m
Ambient temperature, T_a	-5.0, -10 °C
Exposure time, t_{exp}	1 hour
Ambient pressure, p_∞	95610 Pa
Humidity	100 %

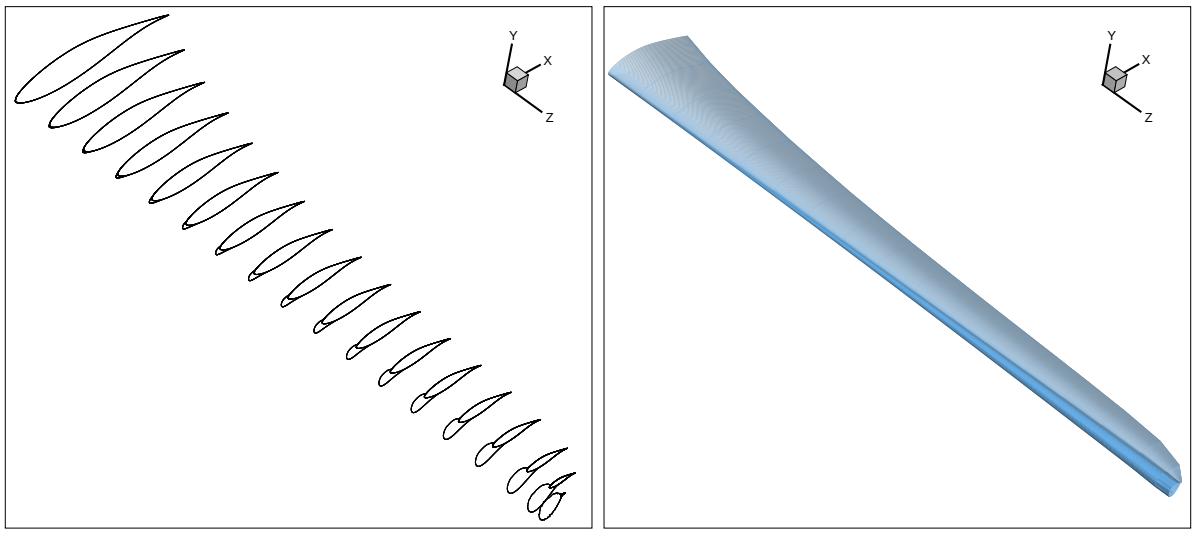

Figure 5: Predicted iced blade element profiles for for Aelos 30 kW wind turbine for conditions in Table 2 (d_p=27 μm, ρ_a=0.05 g/m^3 and t_{exp}=60 mins)

Predicted ice shapes for different span-wise locations can be seen in Figure 5. The shape grows with increasing span due to the increasing sectional velocity and decreasing sectional chord length. Results

show that the change caused by ice accretion degrads the aerodyanmic performance of the blade, especially near the tip section.

CONCLUSION

In this study, ice accretion on wind turbine blades is investigated under atmospheric icing conditions. Obtained preliminary results are analyzed and commented. Ice accretion code predicted ice shape on the blade sections rather well.

The results show that predicted ice shapes at low temperatures are quite similar and exhibit rime ice characteristics. These results conform with expectations since rime ice typically occurs at low temperatures and low liquid water contents while high temperature yields a glaze shape. It is seen that predicted ice shape grows with increasing span due to the increasing sectional velocity and decreasing sectional chord length. Results show that the change caused by ice accretion degraded the aerodynamic performance of the blade.

The presented results show preliminarily that the above methods are feasible for investigating aerodynamic performance losses in both rime and glaze ice conditions to estimate energy production losses of the wind turbines.

References

Barber S., Wang Y., Jafari Y., Chokani N. and Abhari R. S., (2011). *The Impact of Ice Formation on Wind Turbine Performance and Aerodynamics*, Journal of Solar Energy Engineering, Vol.133/011007-1

IEA Wind, (2015). *Wind Energy in Cold Climates*, IEA Wind $R, D\&D$ Task 19, `http://arcticwind.vtt.fi/`, date of access April 23, 2015.

Jasinski, W.J. and Noe, S.C. and Selig, M.S. and Bragg, M.B., (1998). *Wind Turbine Performance Under Icing Conditions*, ASME, Vol.120, pp. 60-65

Makkonen L., Laakso T, Marjaniemi M, Finstad K.J., (2001). *Modelling and Prevention of Ice Accretion on Wind Turbines*, Wind Engineering Volume 25, No:1.

Myers G. Tim, (2001). *Extension to the Messinger Model for Aircraft Icing*, AIAA JOURNAL, Vol. 39, No:2.

Navigant Research (2015). *World Market Update 2013*, `http://www.navigantresearch.com/research/world-market-update-2013`, date of access April 23, 2015.

Ozgen S., Canibek M., (2010). *In Flight Icing Simulation with Supercooled Large Droplet Effects*, 7th Int. Conference on Heat Transfer, Fluid Mechanics and Thermodynamics, Antalya, Turkey.

Ozgen S., Canibek M., (2009). *Ice Accretion Simulation on Multi-Element Airfoils using Extended Messinger Model* , Heat Mass Transfer, Volume 45, Issue 3, pp 305-322.

Parent Oliver, Ilinca Adrian, (2011). *Anti-icing and De-icing Techniques for Wind Turbines: Critical Review*, Cold Regions Science and Technology, 65 (2011) 88-96.

Talhaug L, Vindteknik K, Ronsten G, Horbaty R, Baring-Gould I, Lacroix A, et al., (2007). *Wind Energy Projects in Cold Climates*, 1st ed. Executive Committee of the International Energy Agency Program for Research and Development on Wind Energy Conversion Systems; 2005; submitted for publication. p. 1–36, `http://virtual.vtt.fi/virtual/arcticwind/reports/recommendations.pdf`, date of access April 20, 2015.

Drela M., (2017). *XFOIL [web]*, URL:$http://web.mit.edu/drela/Public/web/xfoil/$, [cited 04 March 2017]

VTT, (2017). WIceAtlas [web], URL:$http://www.vtt.fi/sites/wiceatlas/methodology$, [cited 19 March 2017]